
This is an electronic reprint of the original article.
This reprint may differ from the original in pagination and typographic detail.

Author(s): Qu, Zengcai & Hinkkanen, Marko

Title: Loss-minimizing control of synchronous reluctance motors A review

Year: 2013

Version: Post print

Please cite the original version:

Qu, Zengcai & Hinkkanen, Marko. 2013. Loss-minimizing control of synchronous reluctance motors A review. 2013 IEEE International Conference on Industrial Technology (ICIT). 6. ISBN 978-1-4673-4568-2 (electronic). DOI: 10.1109/icit.2013.6505697.

Rights: © 2013 Institute of Electrical & Electronics Engineers (IEEE). Permission from IEEE must be obtained for all other uses, in any current or future media, including reprinting/republishing this material for advertising or promotional purposes, creating new collective works, for resale or redistribution to servers or lists, or reuse of any copyrighted component of this work in other work.

All material supplied via Aaltodoc is protected by copyright and other intellectual property rights, and duplication or sale of all or part of any of the repository collections is not permitted, except that material may be duplicated by you for your research use or educational purposes in electronic or print form. You must obtain permission for any other use. Electronic or print copies may not be offered, whether for sale or otherwise to anyone who is not an authorised user.

Loss-Minimizing Control of Synchronous Reluctance Motors — A Review

Zengcai Qu and Marko Hinkkanen
Aalto University School of Electrical Engineering
P.O. Box 13000, FI-00076 Aalto, Finland

Abstract—This paper reviews state-of-the-art loss-minimizing control strategies for synchronous reluctance motors. Methods can be categorized as loss-model controllers (LMCs) and search controllers (SCs). For LMCs, different loss models and the corresponding optimal solutions are summarized. The effects of the core losses and magnetic saturation on the optimal stator current are investigated; magnetic saturation is a more important factor than the core losses. For SCs, different search algorithms are presented and compared. The SCs are evaluated based on their convergence speed, parameter sensitivity, accuracy, and the torque ripple caused by the search process.

Index Terms—Core losses, drive, efficiency optimization, energy, loss minimization, magnetic saturation, synchronous reluctance motor.

I. INTRODUCTION

The synchronous reluctance motor (SyRM) is known to be an attractive alternative to other AC machines in variable speed drives [1], [2]. An optimal selection of the stator current vector can minimize the total electrical losses in the motor. The loss-minimizing control of the induction motor suffers from slow dynamic response due to the relatively large rotor time constant [3]. On the other hand, the dynamic performance of the SyRM is not significantly deteriorated due to the loss minimization, since the stator flux linkage is proportional to the stator current.

At lower speeds, the core losses are negligible compared to the copper losses. Therefore, maximum torque-per-ampere (MTPA) methods, which minimize the copper losses, are popular [4]. If magnetic saturation is omitted, the 45-degree current angle (with respect to the d axis) yields the MTPA operation. However, magnetic saturation and parameter variations usually lead to an optimal current angle larger than 45 degree [5], [6]. At higher speeds, the proportion of the core losses increases, and they have to be taken into account as well in order to minimize the total electrical losses of the motor.

Loss-minimizing control methods can be categorized as loss-model controllers (LMCs) and search controllers (SCs). The LMCs apply a loss function, which depends on motor parameters and knowledge of the operating point. The loss-minimizing solution for the angle of the stator-current vector is obtained by minimizing the loss function. Analytical solution can be found, if the loss function is simple enough. However, taking the core losses and magnetic saturation into account leads typically to a very complicated loss function, and the optimal angle has to be determined by numerical searching (either online or off-line).

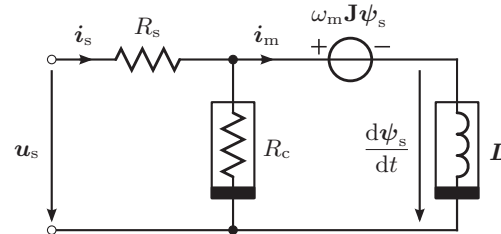


Fig. 1. Dynamic space-vector model of a SyRM in rotor coordinates. The nonlinear inductor can be defined, e.g., $\mathbf{L} = \mathbf{L}(\psi_s)$, and for linear magnetics, it reduces to $\mathbf{L} = \text{diag}(L_d, L_q)$. The core-loss resistor R_c may depend on the stator flux and its frequency.

The SCs adjust the control variable (typically the d-axis current) online based on the feedback from the input power measurement. The SCs are insensitive to model inaccuracies and parameter variations. If the input power of the converter is measured and used as a feedback signal, the converter losses are automatically taken into account. However, typical disadvantages of the SCs are the slow convergence speed and unexpected losses and torque disturbances due to the adjustments of the control variable during the search process.

Much research in the field of energy-efficiency control of SyRMs has been conducted, but no survey on this topic has been available. This paper attempts to review relevant publications in this area and summarize their key results. The SyRM model is briefly described in Section II. Different loss models and the corresponding optimal solutions of various LMCs are discussed in Section III. The effects of the core losses and magnetic saturation on the optimal stator-current angle are analyzed in Section IV. In Section V, SCs are evaluated based on their convergence speed, torque disturbances, and stability of the search algorithms. Finally, Section VI concludes the paper.

II. SYRM MODEL

The d-axis of the rotating coordinate system is defined as the direction of the maximum inductance. Real space vectors will be used in the model. For example, the stator-current vector is $\mathbf{i}_s = [i_{sd}, i_{sq}]^T$, where i_{sd} and i_{sq} are the components of the vector and the matrix transpose is marked with the superscript T. The magnitude is denoted by

$$i_s = \sqrt{i_{sd}^2 + i_{sq}^2} \quad (1)$$

Per-unit quantities will be used.

The dynamic equivalent circuit of the SyRM in rotor coordinates is illustrated in Fig. 1. The stator-voltage equation is

$$\frac{d\boldsymbol{\psi}_s}{dt} = \mathbf{u}_s - R_s \mathbf{i}_s - \omega_m \mathbf{J} \boldsymbol{\psi}_s \quad (2)$$

where $\boldsymbol{\psi}_s$ is the stator-flux vector, \mathbf{u}_s the stator-voltage vector, R_s the stator resistance, ω_m the electrical angular speed of the rotor, and the orthogonal rotation matrix $\mathbf{J} = \begin{bmatrix} 0 & -1 \\ 1 & 0 \end{bmatrix}$.

The core-loss resistance is R_c , and the current $\mathbf{i}_c = \mathbf{i}_s - \mathbf{i}_m$ flows through it. The magnetizing current \mathbf{i}_m is a nonlinear function of the flux due to magnetic saturation (cf. e.g. [7] and references therein):

$$\mathbf{i}_m = \mathbf{i}_m(\boldsymbol{\psi}_s) = \begin{bmatrix} \psi_{sd}/L_d(\psi_{sd}, \psi_{sq}) \\ \psi_{sq}/L_q(\psi_{sd}, \psi_{sq}) \end{bmatrix} \quad (3)$$

where the d- and q-axis inductance functions are denoted by L_d and L_q , respectively.¹

In steady state, the power balance of the SyRM model is given by

$$P_{in} = P_{Cu} + P_{Fe} + T_e \omega_m \quad (4)$$

where the power fed to the stator is $P_{in} = \mathbf{u}_s^T \mathbf{i}_s$ and the electromagnetic torque is

$$T_e = \mathbf{i}_m^T \mathbf{J} \boldsymbol{\psi}_s = i_{mq} \psi_{sd} - i_{md} \psi_{sq} \quad (5)$$

The copper losses are $P_{Cu} = R_s i_s^2$ and the core losses are $P_{Fe} = R_c i_c^2$.

In steady state, the stator core losses can be modeled as

$$P_{Fe} = k_h |\omega_m| \psi_s^2 + k_e \omega_m^2 \psi_s^2 \quad (6)$$

where k_h and k_e are the hysteresis and eddy-current coefficients, respectively. The first term in (6) corresponds to the hysteresis losses and second term corresponds to the eddy-current losses. The core-loss resistance corresponding to (6) becomes

$$R_c = \frac{1}{k_h/|\omega_m| + k_e} \quad (7)$$

It can be seen that the core-loss resistance R_c is constant if the hysteresis losses are omitted ($k_h = 0$).

III. LOSS-MODEL CONTROLLERS

For a given torque and speed, LMCs aim to minimize the input power P_{in} given in (4), or, equivalently, to minimize the losses $P_{loss} = P_{Cu} + P_{Fe}$. The loss function is formulated based on the motor model. The accuracy and the complexity of the solution depend significantly on the modeling assumptions.

¹Alternatively, the saturation can be modeled as

$$\boldsymbol{\psi}_s = \boldsymbol{\psi}_s(\mathbf{i}_m) = \begin{bmatrix} L_d(i_{md}, i_{mq}) i_{md} \\ L_q(i_{md}, i_{mq}) i_{mq} \end{bmatrix}$$

Both forms will be used in the rest of the paper.

A. Constant R_c , L_d , and L_q

In [8], [9], a simple LMC was proposed. The constant core-loss resistance R_c and constant inductances L_d and L_q have been assumed. The sum of the copper losses and the core losses is given by

$$\begin{aligned} P_{loss} &= P_{Cu} + P_{Fe} \\ &= \left[R_s + (R_s + R_c) \frac{\omega_m^2 L_d^2}{R_c^2} \right] i_{md}^2 \\ &\quad + \left[R_s + (R_s + R_c) \frac{\omega_m^2 L_q^2}{R_c^2} \right] i_{mq}^2 \\ &\quad + \left[\frac{2R_s}{R_c} \omega_m (L_d - L_q) \right] i_{md} i_{mq} \end{aligned} \quad (8)$$

From this loss function, the optimal ratio of the current components can be solved as

$$\zeta_{opt} = \frac{i_{mq,opt}}{i_{md,opt}} = \sqrt{\frac{R_s R_c^2 + (R_s + R_c) \omega_m^2 L_d^2}{R_s R_c^2 + (R_s + R_c) \omega_m^2 L_q^2}} \quad (9)$$

which results in $\zeta_{opt} > 1$ since $L_d > L_q$. Therefore, the optimal current angle is slightly larger than 45 degree at all speeds and torques. Since constant inductances have been assumed, (9) does not depend on the torque. In order to simplify the implementation, $i_{sq,opt}/i_{sd,opt} = \zeta_{opt}$ may be assumed. In [10], an approximation of (9) avoiding taking the square root is proposed.

In [11], the solution (9) was implemented, and the core-loss resistance and the inductances are estimated by extended Kalman filter. Since the parameter estimation needs time to converge to actual machine parameters, the loss-minimizing method works well in steady state but not in dynamic loss minimization.

Feedback linearization is applied in [12] to minimize the losses. This method can also be categorized as a LMC. The operating points are assumed to be unsaturated and the saturation effects are not considered. The power losses are minimum if the torque curve and power-loss curve are tangential. Hence, the loss-minimizing points can be solved from

$$\|\nabla T_e(i_{sd}, i_{sq})\| \cdot \|\nabla P_{loss}(i_{sd}, i_{sq})\| \cdot \sin \theta = 0 \quad (10)$$

where ∇T_e is the gradient of electromagnetic-torque curve, ∇P_{loss} is the gradient of the loss curve, and θ is the angle between $\nabla T_e(i_{sd}, i_{sq})$ and $\nabla P_{loss}(i_{sd}, i_{sq})$.

Neural networks (NNs) and fuzzy logic have been used in the LMCs. In [13], a NN is used as an adaptive model of the SyRM. The NN is trained online, and the input is the torque reference and outputs are the d-q axes currents references. The problem in the method is that the NN only maps the relationship between torque and optimal current without taking the rotation speed into account. However, based on (9), the optimal current depends on the rotation speed. Therefore, the NN should also have the rotation speed as an input to identify the optimal d-q axes currents. The LMC proposed in

[14] applies learning mechanism-fuzzy neural networks (LM-FNN). In [15], the loss function (8) is applied, and an offline-trained NN is used to map the optimal current. The saturation effect is compensated for in torque control but not in the loss minimization.

B. Effect of the Hysteresis Losses

In [16], the core losses are modeled according to (6). The loss function is the sum of the core losses and copper losses. The optimal d-axis current is expressed as

$$i_{sd,opt} = \left[\frac{\omega_m^2 L_q^2 + R_s R_c}{\omega_m^2 L_d^2 + R_s R_c} \left(\frac{T_e}{L_d - L_q} \right)^2 \right]^{1/4} \quad (11)$$

where the core-loss resistance R_c is the function (7).

The stray-load losses are taken into account in the total loss function in [17] and [18]. The total loss function considering the hysteresis, eddy-current, and stray-load losses is given by

$$P_{loss} = a(i_{sd}^2 + i_{sq}^2) + b \left[\left(\frac{L_d}{L_q} \right)^2 i_{sd}^2 + i_{sq}^2 \right] \quad (12)$$

where

$$a = R_s + k_s \omega_m^2, \quad b = k_c \omega_m^\beta L_q^2 \quad (13)$$

where k_s , k_c , and β are the parameters of the core-loss model. The loss-minimizing current $i_{sd,opt}$ is given as

$$i_{sd,opt} = i_{sq} \sqrt{\frac{a+b}{a+b(L_d/L_q)^2}} \quad (14)$$

The solution (14) is not directly applied but it is rewritten as

$$i_{sd,opt} = i_{sq} \sqrt{\frac{1 + \omega_m^2 T_1^2}{1 + \omega_m^2 T_2^2}} \quad (15)$$

where T_1 and T_2 are combined functions of the motor parameters. T_1 and T_2 are identified experimentally by input power measurements.

C. Effect of Magnetic Saturation

For LMCs, magnetic saturation is one of the key issues to be considered. However, many loss-minimizing methods in the literature omit the saturation effects and use constant inductances for simplicity. However, the variation of the inductances significantly affects the optimal current angle.

The saturation characteristics of the d-axis and q-axis inductances are different because the d-axis is iron dominating and q-axis is air dominating. Hence, the variation of L_d is more severe. If high accuracy is not required, it may be sufficient to model the saturation effect of the d-axis inductance only.

Various explicit magnetic saturation models can be found in the literature [7]. For example, a power function model is given by

$$L_d(\psi_d) = \frac{L_{du}}{1 + (\alpha|\psi_d|)^a} \quad (16)$$

Arctangent functions, piecewise functions, and polynomial functions have also been used to model the saturation effects.

More precise models of saturation take also the cross coupling between the two axes into account. For example, the model given in [19] is

$$L_d(i_{md}, i_{mq}) = L_{d0}(i_{md}) - L_{d1}(i_{md})L_{q2}(i_{mq}) \quad (17a)$$

$$L_q(i_{md}, i_{mq}) = L_{q0}(i_{mq}) - L_{q1}(i_{mq})L_{d2}(i_{md}) \quad (17b)$$

where L_{d0} , L_{d1} , L_{d2} , L_{q0} , L_{q1} , and L_{q2} are all expressed as rational functions. As an example, the function

$$L_{d0}(i_{md}) = A + \frac{B}{i_{md}^4 + C i_{md}^2 + D} \quad (18)$$

where A , B , C , and D are constant parameters.

The saturation curves are nonlinear functions, which make the loss function much more complicated and difficult to derive an analytical solution for the loss-minimizing current. However, numerical methods can be applied to find the optimal points of the loss function.

There are only a few LMCs considering both core losses and cross-magnetic saturation. In [20], the inductances are measured and fitted to (17). The LMC is based on a repetition function by which the optimal current reference is searched numerically. Based on the results, this seems to be a good solution for high-accuracy loss minimization (if the parameter identification of the model does not cause problems).

IV. PARAMETER SENSITIVITY OF LMCs

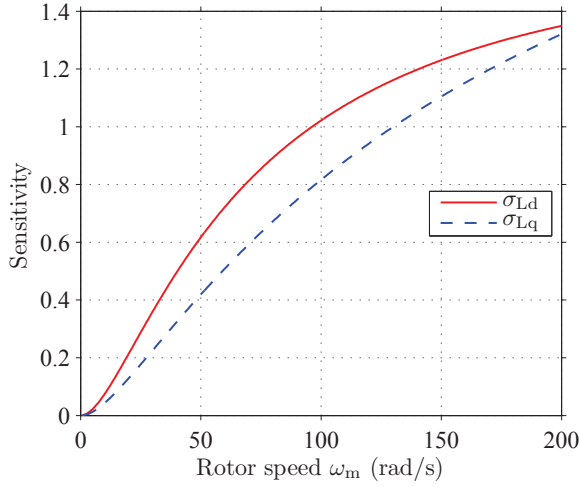
In [21], parameter sensitivity of the LMC corresponding to (9) is studied. The sensitivity functions are defined as differentiation for each motor parameters:

$$\begin{aligned} \sigma_{Ld} &= \frac{\partial \zeta_{opt}}{\partial L_d}, & \sigma_{Lq} &= \frac{\partial \zeta_{opt}}{\partial L_q} \\ \sigma_{R_s} &= \frac{\partial \zeta_{opt}}{\partial R_s}, & \sigma_{R_c} &= \frac{\partial \zeta_{opt}}{\partial R_c} \end{aligned} \quad (19)$$

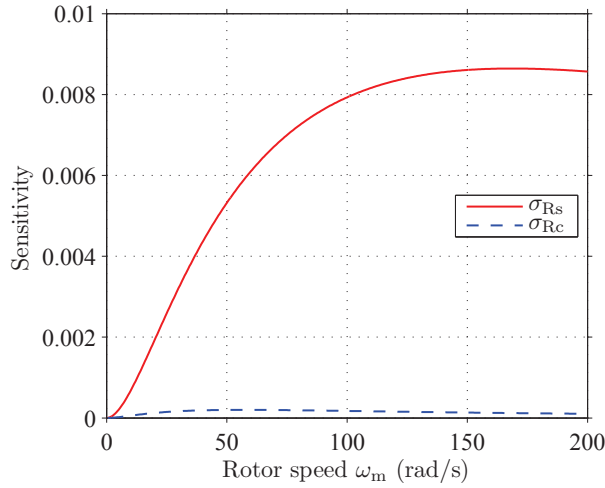
Fig. 2 shows the parameter sensitivities calculated according to (19) using the original motor parameters in [21]. It can be seen that the sensitivities of the parameters have a relationship of $\sigma_{Ld} > \sigma_{Lq} \gg \sigma_{R_s} > \sigma_{R_c}$, which means that the variations of the inductances have more significant influence on the optimal current angle. Furthermore, the variation of L_d is much larger than the variation of L_q .

Fig. 3 shows calculated loss curves of a transverse-laminated 6.7-kW four-pole SyRM with and without the core-loss and saturation models. The rated values of the SyRM are: speed 3175 r/min; frequency 105.8 Hz; line-to-line rms voltage 370 V; rms current 15.5 A; and torque 20.1 Nm. In order to model the inductances as a function of the current, the measured inductance data, cf. [7], were fitted to the model in (17). The core losses are modeled as a constant R_c which is identified by no-load measurement. For simplicity, the average value $R_c = 2.24$ p.u. is used, despite the variation in the actual R_c .

From the results shown in Fig. 3, it is obvious that the core losses increase the total losses but do not affect the optimal current significantly. On the other hand, the saturation effects have more significant influence on the optimal current.



(a)



(b)

Fig. 2. Parameter sensitivity of loss minimization. Results are obtained using the parameters of the motor in [21]. (a) Parameter sensitivity of the inductances; (b) Parameter sensitivity of the stator resistance and the core-loss resistance.

TABLE I
PHENOMENA INCLUDED IN LOSS FUNCTIONS OF LMCs

Publications	Core losses	Magnetic saturation
[6], [8]–[12], [14]–[16]	yes	no
[17], [18]	yes (with stray losses)	no
[22]	no	yes
[19], [20]	yes	yes

The LMCs are categorized in Table I according to phenomena included in loss functions. It can be seen that most of the research has been focused on the effects of the core losses.

V. SEARCH CONTROLLERS

The SCs can be classified into three categories based on their search algorithms: discrete search, continuous search, and signal-injection method. This classification is illustrated in Fig. 4.

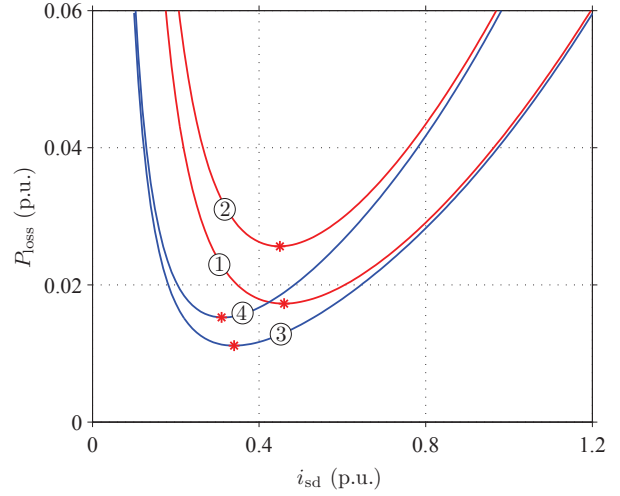


Fig. 3. Losses as a function of the d-axis current at $T_e = 0.5T_N$ and $\omega_m = 0.2$ p.u. The explanation of the curves are: ① without core losses and without magnetic saturation; ② with core losses and without magnetic saturation; ③ without core losses and with magnetic saturation; ④ with both core losses and magnetic saturation. The losses are plotted using the parameters of a 6.7-kW SyRM, whose magnetic saturation is modeled as in [19] and core losses are modeled as a constant resistance R_c .

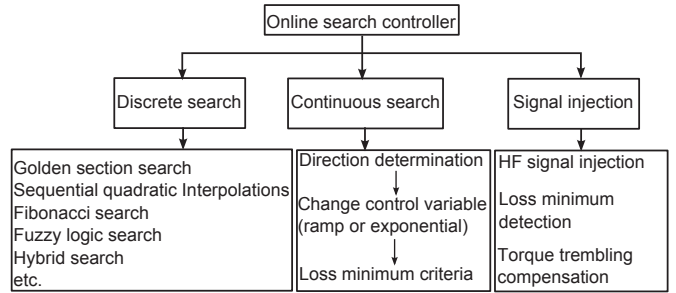


Fig. 4. Categories of SCs.

A. Discrete Search

In discrete search methods, the control variable is changed in steps. Based on the measured (or estimated) input power, new values of the control variable are selected, and the search method iteratively approaches to the optimal point using a minimum search algorithm.

In [16], the d-axis current reference is decreased five steps and then increased ten steps and the input power is measured at each step. Then, the SC adjusts the current reference to the level where the input power has the minimum value and repeats this kind of search procedure. The current reference is changed up and down for the purpose of tracking the minimum input power operating point. This method is simple and easy to apply, but it is inefficient. For example, if the disparity between the optimal current and the actual current is $10\Delta i_d$ (Δi_d is the current step), the method needs 30 steps (10 down and 20 up) to reach the new optimal value. If the current step is large, it will cause torque disturbances. Furthermore, the d-axis current still keeps changing up and down in steady state, where the speed and load are constant. This variation around

the optimal current will also cause torque ripple and additional losses.

In [23], the SC is implemented using the Fibonacci search algorithm. The Fibonacci search is known as an efficient search method for the minimum of a unimodal function in an interval. The Fibonacci search algorithm can precisely find the minimum point. However, it searches the whole current range, which means that very high and low currents are also searched. This causes torque ripple and high losses during the search procedure. However, for the loss-minimizing control, an approximate optimal point can be determined by a rough model (with or without the core losses and saturation model). The loss function is known to be a concave function with only one minimum point. Therefore, in order to make the search faster and reduce the torque ripple, initial values can be strategically selected for this search algorithm.

The SC proposed in [24] applies adaptive fuzzy logic for the first part of the search and the golden-section search method in the second part. The efficiency optimization strategy using fuzzy logic can speed up the search process. The fuzzy logic search changes the current in the direction in which the input power is reduced. When the input power starts to increase, the search method switches to the golden-section search, which can find the minimum point. Comparing with the Fibonacci search in [23], the hybrid search method with fuzzy logic can speed up the search procedure and reduce the steps needed.

In [25], the SC is implemented using the sequential quadratic interpolations. This method iteratively approaches to the optimal point assuming that the loss function is quadratic. Experimental results show that the method converges to the optimal flux with only a few iterations.

In [26], Steady state power losses are minimized by using a fuzzy logic search control system and the LMC is used during transient states. The fuzzy logic search control combines two fuzzy logic controllers: one decreases the d-axis current and the other increases the d-axis current in steps.

B. Continuous Search

Continuous search methods increase or decrease the control variable in a continuous manner instead of stepwise changes. The input power measurements are taken in a time window. The control variable is changed to the direction in which the input power is reduced. When the input power starts to increase or the derivative of input power with respect to the control variable is zero, the optimal point has been found.

In [27], the control variable is the d-axis current, which follows a ramp trajectory. The difference of the input power is measured at the beginning and at the end of the moving window. In this manner, torque disturbances become smoother than in discrete search methods.

In [28], the loss minimization algorithm consists of three steps: 1) detect transient or steady state by the speed error; 2) determine the direction towards the loss-minimizing point; 3) change the control variable to the loss-minimizing direction and determine the minimum-loss condition. The flux is

changed incrementally (or decrementally) in an exponential manner.

C. Signal Injection

The SC based on signal injection was proposed in [29], where the current angle θ yielding zero input power variation in steady state is searched for. In other words, the loss-minimizing criterion is $\partial P_{in}/\partial\theta = 0$, where P_{in} is the input power. A high-frequency excitation signal is superimposed on the current angle. The response in the input power caused by the injected signal is monitored, and the loss-minimizing current angle is tracked based on this response. The convergence to the optimal current angle takes a few seconds.

VI. CONCLUSION

This paper reviewed loss-minimizing control methods of the SyRM. The LMCs are faster and have smaller disturbances in the torque than the SCs. The disadvantage of the LMCs is their dependence on motor parameters. The core losses and magnetic saturation are the most important phenomena to be considered in the LMCs. Based on parameter sensitivity analysis, it is especially important to take magnetic saturation into account in the LMCs.

The SCs minimize the input power based on the real-time power measurement. Hence, the loss model is not needed, and errors due to the parameter variations and modeling inaccuracies are avoided. In this review, the SCs were divided into three categories based on the searching algorithms: discrete search, continuous search, and signal-injection based methods. Typical disadvantages of the SCs are that the search process causes torque ripple and the convergence speed is not sufficient for dynamic applications.

REFERENCES

- [1] A. Boglietti and M. Pastorelli, "Induction and synchronous reluctance motors comparison," in *Proc. IEEE IECON 2008*, Orlando, FL, Nov. 2008, pp. 2041–2044.
- [2] H. Lendenmann, R. R. Moghaddam, A. Tammi, and L.-E. Thand, "Motoring ahead—synchronous motors controlled by variable-speed drives are bringing higher efficiencies to industrial applications," *ABB Review*, no. 1, pp. 56–61, 2011.
- [3] Z. Qu, M. Ranta, M. Hinkkanen, and J. Luomi, "Loss-minimizing flux level control of induction motor drives," *IEEE Trans. Ind. Appl.*, vol. 48, no. 3, pp. 952–961, May/Jun. 2012.
- [4] Y. Inoue, S. Morimoto, and M. Sanada, "A novel control scheme for maximum power operation of synchronous reluctance motors including maximum torque per flux control," *IEEE Trans. Ind. Appl.*, vol. 47, no. 1, pp. 115–121, Jan.-Feb. 2011.
- [5] L. Xu, X. Xu, T. A. Lipo, and D. W. Novotny, "Vector control of a synchronous reluctance motor including saturation and iron loss," *IEEE Trans. Ind. Appl.*, vol. 27, no. 5, pp. 977–985, Sep./Oct. 1991.
- [6] J. E. Fletcher, B. W. Williams, and T. C. Green, "Loss reduction in a synchronous reluctance drive system using DSP control," in *Proc. IEEE PESC'95*, Atlanta, GA, Jun. 1995, pp. 402–407.
- [7] Z. Qu, T. Tuovinen, and M. Hinkkanen, "Inclusion of magnetic saturation in dynamic models of synchronous reluctance motors," Marseille, France, Sept. 2012, pp. 992–998.
- [8] S.-J. Kang and S.-K. Sul, "Efficiency optimized vector control of synchronous reluctance motor," in *Conf. Rec. IEEE-IAS Annu. Meeting*, vol. 1, San Diego, CA, Oct. 1996, pp. 117–121.
- [9] J. H. Mun, J. S. Ko, J. S. Choi, M. G. Jang, and D. H. Chung, "Efficiency optimization control of SynRM drive using multi-AFLC," in *Proc. ICEMS'10*, Incheon, South Korea, Oct. 2010, pp. 908–913.

- [10] F. Fernandez-Bernal, A. Garcia-Cerrada, and R. Faure, "Efficient control of reluctance synchronous machines," in *Proc. IEEE IECON'98*, vol. 2, Aachen, Germany, Aug./Sep. 1998, pp. 923–928.
- [11] T. Senjyu, K. Kinjo, N. Urasaki, and K. Uezato, "High efficiency control of synchronous reluctance motors using extended Kalman filter," *IEEE Trans. Ind. Electron.*, vol. 50, no. 4, pp. 726–732, Aug. 2003.
- [12] H.-D. Lee, S.-J. Kang, and S.-K. Sul, "Efficiency-optimized direct torque control of synchronous reluctance motor using feedback linearization," *IEEE Trans. Ind. Electron.*, vol. 46, no. 1, pp. 192–198, Feb. 1999.
- [13] T. Senjyu, T. Shingaki, A. Omoda, and K. Uezato, "High efficiency drives for synchronous reluctance motors using neural network," in *Proc. IEEE IECON'00*, Nagoya, Japan, Oct. 2000, pp. 777–782.
- [14] J.-S. Choi, J. S. Ko, K.-T. Park, B.-S. Park, and D.-H. Chung, "Efficiency optimization control of SynRM drive by LM-FNN controller," in *Proc. ICPE'07*, Daegu, South Korea, Oct. 2007, pp. 373–377.
- [15] W.-S. Baik, M.-H. Kim, N.-H. Kim, D.-H. Kim, K.-H. Choi, and D.-H. Hwang, "An optimal efficiency control of reluctance synchronous motor using neural network with direct torque control," in *Proc. IEEE IECON'03*, vol. 2, Roanoke, VA, Nov. 2003, pp. 1590–1595.
- [16] T. Matsuo, A. El-Antably, and T. A. Lipo, "A new control strategy for optimum-efficiency operation of a synchronous reluctance motor," *IEEE Trans. Ind. Appl.*, vol. 33, no. 5, pp. 1146–1153, Sep./Oct. 1997.
- [17] I. Kioskeridis and C. Mademlis, "Energy efficiency optimisation in synchronous reluctance motor drives," *IEE Proc. Electr. Power Appl.*, vol. 150, no. 2, pp. 201–209, Mar. 2003.
- [18] C. Mademlis, I. Kioskeridis, and N. Margaris, "Optimal efficiency control strategy for interior permanent-magnet synchronous motor drives," *IEEE Trans. Energy Convers.*, vol. 19, no. 4, pp. 715–723, Dec. 2004.
- [19] S. Yamamoto, T. Ara, and K. Matsuse, "A method to calculate transient characteristics of synchronous reluctance motors considering iron loss and cross-magnetic saturation," *IEEE Trans. Ind. Appl.*, vol. 43, no. 1, pp. 47–56, Jan. 2007.
- [20] S. Yamamoto, J. Adawey, and T. Ara, "Maximum efficiency drives of synchronous reluctance motors by a novel loss minimization controller considering cross-magnetic saturation," in *Proc. IEEE ECCE'09*, San Jose, CA, Sep. 2009, pp. 288–293.
- [21] T. Senjyu, T. Shingaki, and K. Uezato, "A novel high efficiency drive strategy for synchronous reluctance motors considering stator iron loss in transient conditions," in *Proc. IEEE PESC'01*, vol. 3, Vancouver, Canada, Jun. 2001, pp. 1689–1694.
- [22] C. Mademlis, "Compensation of magnetic saturation in maximum torque to current vector controlled synchronous reluctance motor drives," *IEEE Trans. Energy Convers.*, vol. 18, no. 3, pp. 379–385, Sep. 2003.
- [23] T. Lubin, H. Razik, and A. Rezzoug, "On-line efficiency optimization of a synchronous reluctance motor," *Electric Power Systems Research*, vol. 77, no. 10, pp. 484–493, Apr. 2007.
- [24] S. Yifa, S.-Y. Yu, and Z. Wen-Zhen, "Research on efficiency optimization of interior permanent magnet synchronous motor based on intelligent integrated control," in *Chinese Control and Decision Conference (CCDC)*, Xuzhou, China, May 2010, pp. 3059–3063.
- [25] H. F. Hofmann, S. R. Sanders, and A. EL-Antably, "Stator-flux-oriented vector control of synchronous reluctance machines with maximized efficiency," *IEEE Trans. Ind. Electron.*, vol. 51, no. 5, pp. 1066–1072, Oct. 2004.
- [26] E. S. Sergaki and G. S. Stavrakakis, "Online search based fuzzy optimum efficiency operation in steady and transient states for DC and AC vector controlled motors," in *Proc. ICEM'08*, Vilamoura, Portugal, Sep. 2008, CD-ROM.
- [27] S. Vaez, V. I. John, and M. A. Rahman, "An on-line loss minimization controller for interior permanent magnet motor drives," *IEEE Trans. Energy Convers.*, vol. 14, no. 4, pp. 1435–1440, Dec. 1999.
- [28] H. A. Zarchi, J. Soltani, G. R. A. Markadeh, M. Fazeli, and A. K. Sichani, "Variable structure direct torque control of encoderless synchronous reluctance motor drives with maximized efficiency," in *Proc. IEEE ISIE'10*, Bari, Italy, Jul. 2010, pp. 1529–1535.
- [29] S. Kim, S.-K. Sul, K. Ide, and S. Morimoto, "Maximum efficiency operation of synchronous reluctance machine using signal injection," in *Proc. IPEC-Sapporo'10*, Sapporo, Japan, Jun. 2010, pp. 2000–2004.